

Received May 15, 2020; reviewed; accepted September 09, 2020

Binding features of N-hexadecanoylglycine on two terminations of fluorapatite (001) surface and their effect on fluorapatite flotation

Heng Zou ¹, Dianwen Liu ^{1,2}, Qinbo Cao ^{1,2}, Xiumin Chen ²

¹ Faculty of Land Resources Engineering, Kunming University of Science and Technology, Kunming 650093, Yunnan, PR China

² State Key Laboratory of Complex Nonferrous Metal Resources Clean Utilization, Kunming University of Science and Technology, Kunming 650093, China

Corresponding authors: dianwenliu@kust.edu.cn (Dianwen Liu), qinbocao@kust.edu.cn (Qinbo Cao)

Abstract: N-hexadecanoylglycine (C16Gly) is a newly synthesized collector, which can be used as an efficient collector for fluorapatite (FA) rather than for dolomite. To extend our knowledge regarding the C16Gly collector, the contact angle method was employed to understand the flotation selectivity of C16Gly in the FA and dolomite system. On the other hand, the possible binding models of C16Gly anion on Ca-rich and PO₄-rich terminations of FA (001) surface were investigated with density functional theory calculations to reveal the interaction between the C16Gly and the FA surface. Results showed that C16Gly anion could interact with these two terminations to generate 12 low-energy configurations, including bidentate, tridentate and chelating binding models. The C16Gly anion preferred to adsorb onto the Ca-rich termination, which is caused by the weaker electrostatic repulsion force between the C16Gly anion and the PO₄ groups on this termination. The adsorption of C16Gly on these terminations was more stable than that on the dolomite (104) surface, which is one of the reasons for the preferential flotation of FA from dolomite using C16Gly as a collector. These findings provide further insights into the selectivity of C16Gly during the flotation of FA and dolomite.

Keywords: fluorapatite, adsorption, amino acid-based collector, density functional theory

1. Introduction

The flotation of phosphate has been receiving considerable attention over the past several decades, because phosphate ore is a major resource to produce phosphate fertilizers (Herring and Fantel, 1993; Sis and Chander, 2003).

With the depletion of high-grade phosphate ore, low-grade phosphate ores containing abundant amounts of dolomite (CaMg(CO₃)₂) are becoming important phosphate resources in China. The separation of fluorapatite (FA, Ca₅(PO₄)₃F) from dolomite is a crucial issue, since dolomite can also interact with fatty acid collectors (Pradip et al., 2002; Yu et al., 2016). In the industry, dolomite is separated from FA using a reverse flotation strategy. In this flotation scheme, FA is depressed by H₃PO₄/H₂SO₄, whereas dolomite is floated by fatty acid collectors (Ge et al., 2008). However, given the extremely high dosages of depressors and collectors, the cost of this flotation method is notably high. Therefore, the separation efficiency of FA from dolomite remains to be enhanced.

In this regard, the development of selective collector for phosphate flotation is attracting intensive interest (Bordes and Holmberg, 2011; Hu and Xu, 2003; Karlkvist et al., 2015; Wang et al., 2006). N-hexadecanoylglycine (C16Gly) was recently synthesized and used as a collector for phosphate flotation (Cao et al., 2019). This collector exhibits an equally collecting capability for FA compared with oleate. While, dolomite cannot be floated efficiently by this collector. Such flotation selectivity of C16Gly can be maintained in a wide temperature range (10°C-40°C). Considering the selectivity of C16Gly collector and its tolerance for low temperature, this collector has potential to be used in industries.

The adsorption characteristics of C16Gly on FA and dolomite surfaces are vital factors not only for understanding the selective flotation of this collector but also for designing more selective collectors. Such information at the atomic scale can be directly obtained by computer simulation methods (Pradip and B, 2003; Rai and Pradip, 2012). In recent years, density functional theory (DFT) calculation has become a popular tool to analyze the adsorption of a collector on a mineral surface, by which the adsorption energy and the binding structure of collector on a mineral surface can be probed evidently (Chen et al., 2018; Foucaud et al., 2019a; Geneyton et al., 2020; Zhang et al., 2019). Especially, DFT calculation has been applied to determine the binding features of fatty acids with different chain lengths on the hydrated fluorite surface (Foucaud et al., 2018b). Besides, the adsorption mechanism of Na_2CO_3 and Na_2SiO_3 on the fluorite surface has been revealed successfully by the DFT calculation method (Foucaud et al., 2019b). These theoretical studies for fluorite flotation widen current knowledge of the flotation behavior of calcium-bearing minerals.

In our previous work (Cao et al., 2019), DFT calculations were conducted to investigate the binding behavior of C16Gly on the FA (001) and dolomite (104) surfaces. These surfaces are the cleavage surfaces of FA and dolomite. We observed that the adsorption of C16Gly on the FA surface is more favorable than that on the dolomite surface.

It was noticed that only one termination exists on the dolomite (104) surface. Differently, three terminations exist on the FA (001) surface, commonly termed as Ca-rich, Ca-middle, and PO_4 -rich terminations (Qiu et al., 2017). These terminations can occur on the FA (001) surface during the grinding of FA. In our previous work, the adsorption features of C16Gly on the Ca-middle termination have been well probed with DFT calculations (Cao et al., 2019). However, the steric properties of these terminations are far different from each other. The steric feature of a Ca-bearing mineral surface is a critical factor affecting the adsorption of an amino acid-based collector (Hirva and Tikka, 2002). The Ca-Ca distances and Ca densities on calcium-bearing minerals are different from each other, which affect the adsorption of a depressor or collector on a calcium-bearing mineral surface because these reagents can react with Ca atoms on the mineral surface (Filippov et al., 2018). The surface energies of Ca-rich and PO_4 -rich terminations are relatively higher than that of Ca-middle termination; thus these terminations are more reactive compared with the Ca-middle termination (Qiu et al., 2017). Especially for the Ca-rich termination, owing to the higher Ca density on the surface, the interaction of amino acids on this termination is considerably strong (Almorabarríos et al., 2009). Thus, it is reasonable to predict that the binding features of C16Gly on the Ca-rich and PO_4 -rich terminations of FA (001) surface may deviate notably from that on the Ca-middle termination.

In this regard, the presence of different terminations on the FA (001) surface poses the question of how the steric features of different terminations of FA (001) surface affect the binding of C16Gly on the terminations, and another question is whether the binding strengths of C16Gly on Ca-rich and PO_4 -rich terminations are consistent with the selective flotation of FA with C16Gly. Therefore, the interaction of C16Gly with the Ca-rich and PO_4 -rich terminations should be investigated with DFT calculations.

In this work, aiming to further extend our knowledge regarding the flotation behavior of FA with C16Gly, the possible binding models of C16Gly on two FA (001) surface terminations, i.e., Ca-rich and PO_4 -rich terminations, were revealed using the DFT method. The nature of Ca-O bonds formed on the FA surface was also assessed using the electron density difference analysis. Moreover, the adsorption energies of C16Gly on these two terminations were compared with those on the dolomite surface to further interpret the flotation selectivity of C16Gly in the FA-dolomite system.

2. Materials and methods

2.1. Minerals and reagents

Pure FA and dolomite crystals used in this work were from the Geological Museum of Yunnan Province, China. The C16Gly collector ($\text{CH}_3(\text{CH}_2)_{14}\text{CONHCH}_2\text{COOH}$) was synergized in the chemistry lab of Kunming University of Science and Technology, according to the report of Zhang (Zhang et al., 2005). The NMR results of this collector were presented in our previous work (Cao et al., 2019). Hydrochloric acid and sodium hydroxide are both AR grade and purchased from Sigma Aldrich, which were used to adjust the pH of the collector solution. All the solutions were prepared with deionized (DI) water.

2.2. Contact angle measurements

The contact angles of FA and dolomite surfaces conditioned with C16Gly solutions were measured by a GBX 3S instrument (France). The FA and dolomite crystals were polished with Al₂O₃ sandpapers (2000-, 4000- and 6000-grit) to obtain a fresh and smooth surface. The crystals were treated by the collector solution for 4 min, after which the crystals were air-dried for further measurement. A droplet of DI water (~2mm of diameter) was placed on the dry crystal surface, while the contact angles on both sides of the droplet were measured by the instrument. Each sample was measured by 3 times and the mean value was reported.

2.3. Calculation details

Cambridge Serial Total Energy Package (CASTEP) program was used in DFT calculations (Segall et al., 2002). Perdew-Burke-Ernzerhof functional, a generalized gradient approximation, was selected to treat the exchange and correlation potentials (Perdew et al., 1996; Perdew and Zunger, 1981). The interactions between the ionic core and the valence electrons were described with ultrasoft pseudopotentials (Francis and Payne, 1990). A 440.0 eV of kinetic energy cutoff was used in calculations. The Brillouin-zone integrations were sampled with a 2×2×1 k-point mesh for the FA surface model with a 35 Å of vacuum layer. The cutoff energy and k-point mesh were sufficient for the system as determined by convergence tests.

The surface models and C16Gly anion were optimized with the Broyden-Fletcher-Goldfarb-Shanno (BFGS) procedure (Head and Zerner, 1985). The convergence criteria for structure optimization and energy calculation included (a) an energy tolerance of 1×10⁻⁶ eV/atom, (b) a maximum force tolerance of 0.03 eV/Å, and (c) a maximum displacement tolerance of 0.001 Å. In addition, the C16Gly anion was added in a cubic cell (16×19×45 Å) to calculate the optimal structure, and this process was conducted at the gamma point in the Brillouin zone. The adsorption energy (ΔE_{ads}) due to the interaction of C16Gly with the FA surface was calculated according to:

$$\Delta E_{ads} = E_{collector+surface} - E_{collector} - E_{surface} \quad (1)$$

where $E_{collector+surface}$ and $E_{surface}$ refer to the total energies of the surface model with and without a C16Gly anion, respectively. $E_{collector}$ is the energy of C16Gly anion with -1 e of formal charge. All the atoms in each slab model were allowed to fully relax during the geometry optimization.

3. Results and discussion

3.1. Contact angle tests

The hydrophobicity of a mineral surface is a major factor that determined the flotation behavior of the mineral to some extent. Here contact angle method was employed to probe the hydrophobicity of FA and dolomite surfaces in C16Gly solution, aiming to further examine the flotation selectivity of C16Gly for FA and dolomite system.

Fig. 1 presents the contact angles of FA and dolomite treated by 1×10⁻⁴ mol/dm³ of C16Gly solutions. The contact angles of FA or dolomite were governed by the pH of the C16Gly solution. As for FA, the contact angle was less 30° at pH 3 or 4. When the pH of the collector solution was higher than 5, the contact angle of FA reached 80°. In this pH range, FA could be well floated by C16Gly (Cao et al., 2019). The contact angle and flotation results both imply that C16Gly could adsorb onto the FA surface efficiently at pH>5. In the case of dolomite, because dolomite is not stable in a strongly acidic solution, the pH of C16Gly solution of dolomite in the contact angle measurement was in the region of 5-11. It was found that a moderate contact angle (43°) was obtained by the condition with the C16Gly solution at pH 5. Noted that the contact angle of dolomite decreased with the increase in pH. Further, the contact angle of dolomite was below 20° at pH 9 or 11. Such results indicate that dolomite could not be well floated by C16Gly at pH 9 or 11, which agrees well with the previous flotation results (Cao et al., 2019). Therefore, C16Gly could be employed as an efficient and selective collector for FA at pH 9 or 11 in the FA and dolomite system.

Previous zeta potential results indicated the FA surface was negatively charged at pH 9 or 11 while the adsorption of C16Gly anion on the FA surface further lowered the zeta potential of FA surface

notably (Cao et al., 2019). The pK_a of the carboxylic groups of the amino acids with chain length of C12 was reported in the pH region of 2-4 (Karlkvist et al., 2015). It is reasonable to expect that the pK_a of COOH in C16Gly is in the similar pH region, and the $-COOH$ group in C16Gly may dissociate into $-COO^-$ in an alkaline solution. Thus, C16Gly anion ($C_{15}H_{31}CONHCH_2COO^-$) is generated in the solution to react with the FA surface. The pK_a of C16Gly should be determined by an experimental method in the future.

As stated in the Introduction, the interactions between the C16Gly anion and the PO_4 -rich and Ca-rich terminations of FA (001) surface are important to understand the flotation selectivity of C16Gly. Thus, the binding models of C16Gly anion on these terminations were further revealed by the DFT calculations in the following sections.

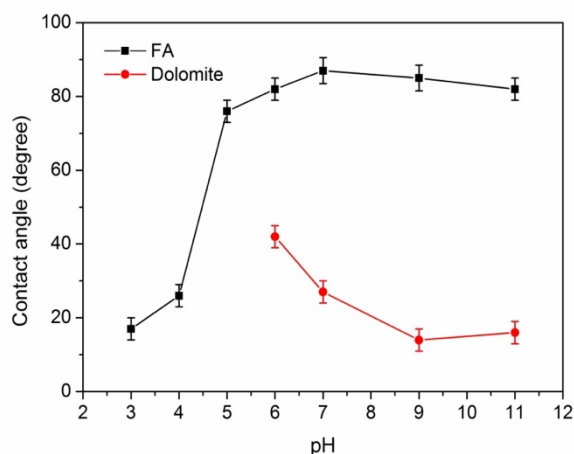


Fig. 1. Contact angles of FA and dolomite treated by 1×10^4 mol/dm³ of C16Gly solutions at different pH

3.2. Chemical properties of C16Gly anion

The chemical properties of C16Gly anion are important factors determining the flotation behavior of this collector. Here, the Mulliken charge population and highest occupied molecular orbital (HOMO) of the C16Gly anion were assessed to understand the chemical reactivity of the C16Gly anion.

Firstly, the Mulliken charge population of C16Gly anion was calculated. Only the results of O and N atoms in the collector were reported as these atoms may bind to the FA surface. The three O atoms in the C16Gly anion were numbered as O1 (the single-bonded O in the carboxyl group), O2 (the double-bonded O in the carboxyl group), and O3 (the O in the amide group), Fig. 2a. It was found that these O atoms and also the N atom in the amide group were all negatively charged in the C16Gly anion. The charge of O1 (-0.72 e) was close to that of O2 (-0.71 e). While the charge of O3 (-0.65e) was only 0.06 e higher compared with that of O2. The binding of C16Gly anion to the FA surface can generate Ca-O bonds (Cao et al., 2019). The Ca-O bond features a high level of ionicity arising from the electrostatic force between O and Ca atoms. Based on the Mulliken charge results, all O atoms in the C16Gly anion are possible to interact with the Ca atoms on the FA surface.

The highest occupied molecular orbital (HOMO) of a collector determines the chemical reactivity of the collector to a certain degree (Peng et al., 2018; Yang et al., 2017). Hence, the HOMO of C16Gly anion was also calculated as plotted in Fig. 2b. The HOMO of C16Gly mainly consisted of the 2p orbitals of O1 and O2. The orbitals of N and O3 exhibited considerably less contribution to the HOMO. It appears that the N and O3 in the C16Gly were less reactive than O1 or O2, although the charges of N and O3 approached that of O1 or O2. It is reasonable to infer that the adsorption of C16Gly on the FA surface mainly depended on the interaction between O1/O2 from C16Gly and the Ca atoms on the FA surface. To verify this claim, the binding models of C16Gly anion on the terminations of FA (001) surface was further calculated by the DFT methods.

3.3. PO_4 -rich and Ca-rich FA (001) terminations

Fig. 3 compares the PO_4 -rich and Ca-rich terminations of the FA (001) surface. In terms of the PO_4 -rich termination, the atoms on the top of the surface were O atoms of PO_4 groups. Differently, in the case of

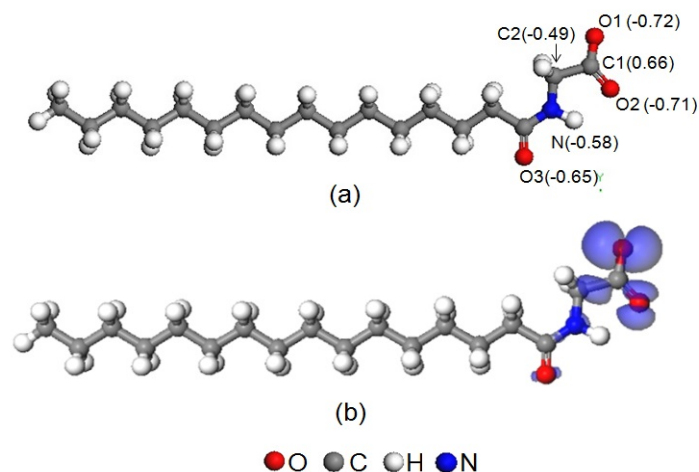


Fig. 2. Chemical features of C16Gly anion: (a) Mulliken charges (e) of selected atoms and (b) HOMO of the C16Gly anion

Ca-rich termination, the first atomic layer on the surface consisted of Ca atoms. While, Ca atoms are also located on the outmost layer of Ca-middle termination (Qiu et al., 2017), but the density of Ca on the Ca-middle termination is less than that on the Ca-rich termination. The Ca densities of three terminations were calculated as 6.5 (PO₄-rich termination), 8.7 (Ca-middle termination) and 10.8 $\mu\text{mol}/\text{m}^2$ (Ca-rich termination) based on their slab models. Therefore, the Ca-rich termination featured the highest Ca density among the three terminations.

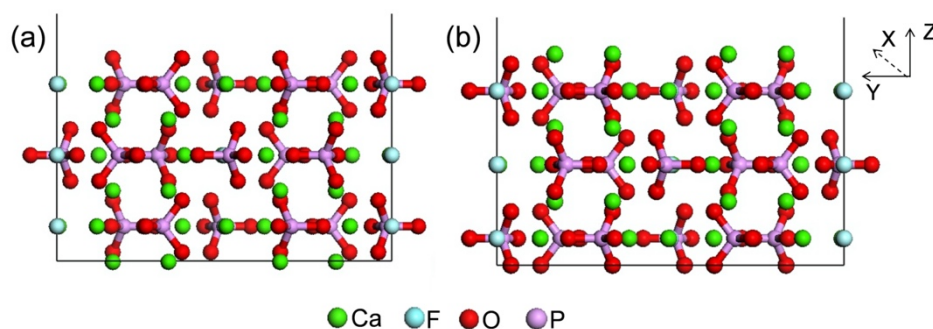


Fig. 3. Two FA (001) surface terminations: (a) PO₄-rich termination; (b) Ca-rich termination

The surface energies of these terminations followed the order of Ca-rich termination > PO₄-rich termination > Ca-middle termination (Qiu et al., 2017). The difference in Ca density and surface energy of these terminations may give rise to variations in the binding structures of C16Gly anion on these terminations. The interaction of C16Gly and the Ca-middle termination has been investigated in detail (Cao et al., 2019). In the present work, we focused on probing the adsorption models of C16Gly anion on the Ca-rich and PO₄-rich terminations.

3.4. Adsorption of C16Gly on the Ca-rich termination

On the optimized Ca-rich termination of the FA (001) surface, the PO₄ groups in the slab model rotated to a certain degree as a result of surface relaxation (Fig. 4a). Noted that the rotation of PO₄ groups in the bottom layer was negligible, indicating that the three-layered structure is large enough to present the FA surface.

Possibly interacting Ca atoms in this slab model were numbered as Ca1–Ca4 atoms (Fig. 4b). These Ca atoms were located in two layers along the z-axis. Ca1 and Ca2 were present at the outmost layer of the surface, whereas Ca3 and Ca4 were in a deeper layer. Surface relaxation also affected the distances between these Ca atoms. Consequently, the distances among possibly interacting Ca atoms increased

by 0.02-0.1 Å (Table 1). It suggests that surface relaxation influenced the steric features of Ca atoms on the top of the Ca-rich termination.

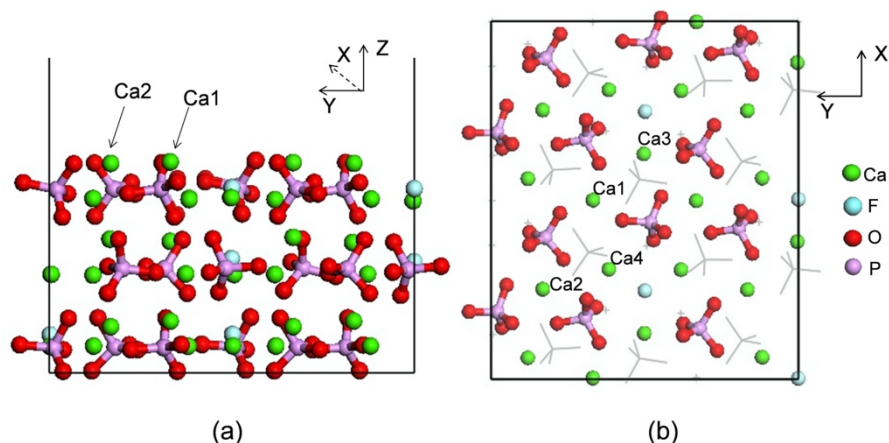


Fig. 4. Optimized Ca-rich termination of FA (001) surface: (a) side view and (b) top view (Bottom atoms are showed in a grey-line style)

Table 1. Distance (Å) between Ca atoms on the Ca-rich termination of FA(001) surface before and after the geometry optimization

	Ca1-Ca2	Ca1-Ca3	Ca2-Ca4
Before	5.44	3.96	4.08
After	5.54	4.09	4.10

C16Gly anion could adsorb on this Ca-rich termination in seven models (Fig. 5). These binding models can be classified into the following three types: bidentate binding (bi1–bi3), tridentate binding (tri1–tri3) and chelating binding (ch1) structures. As shown in Fig. 5a, the O1 and O2 in C16Gly anion could interact with Ca2 and Ca1, respectively, forming a bidentate binding structure (bi1 structure). The C16Gly anion could also bind to Ca1 and Ca2 in a reverse structure (bi2 structure), where O1–Ca1 and O2–Ca2 bonds were formed (Fig. 5b). In the bi3 structure, the C16Gly anion connected with Ca1 and Ca3 atoms (Fig. 5c). Meanwhile, the C16Gly anion could interact with two Ca atoms on the Ca-rich termination via three Ca–O bonds. As shown in Fig. 5d, the O1 and O2 in C16Gly anion were coordinated to Ca1 and Ca3, generating three O–Ca bonds (tri1 structure). The C16Gly anion could also interact with Ca2 and Ca4 atoms in two different ways, generating tri2 and tri3 structures (Figs. 5e and 5f). In addition, the O1 and O2 atoms could bind with the Ca1 atom, generating a surface chelate complex (Fig. 5g). It was observed that H-bonds between NH and PO₄ groups occurred in the tri2 and tri3 models, thereby aiding in the adsorption of C16Gly onto the FA surface.

Notably, in all the binding structures, the O3 atom in the C16Gly anion was uninvolved in the surface reaction. A similar result was also found on the Ca-middle termination of the FA (001) surface (Cao et al., 2019). It appears that the O3 atom was less reactive than O1 and O2 atom during the surface interaction. This result agrees with the above HOMO analysis of C16Gly anion.

The bond angle of O1–C1–O2 was 130.52° in the free C16Gly anion, and it decreased by 2.9°–6.1° due to the interaction between the C16Gly anion and the surface (Table 2). On the other hand, the adsorption energies were all negative and ranged from -281.1 kJ/mol to -195.2 kJ/mol (Table 2), indicating that it is energetically favorable for the C16Gly anion to adsorb on the Ca-rich terminated surface. Further, the bi1 structure was the most stable structure due to its lowest adsorption energy.

3.5. Adsorption of C16Gly on PO₄-rich termination

Fig. 6a presents the optimized slab model of the PO₄-rich termination of FA (001) surface. The PO₄ groups in this model scarcely rotated after the surface relaxation. Three Ca atoms on the top of this termination, noted as Ca5, Ca6 and Ca7 atoms, could react with the C16Gly anion (Fig. 6b). The distan-

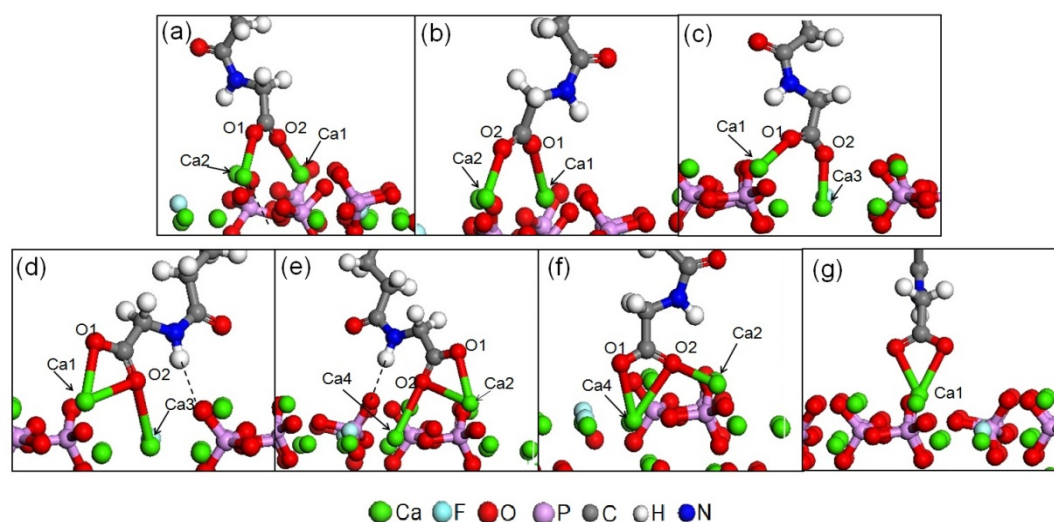


Fig. 5. Binding models of C16Gly anion on the Ca-rich termination of FA (001) surface: (a) bidentate binding with Ca1 and Ca2 (bi1); (b) bidentate binding with Ca1 and Ca2 in a reverse pattern from the bi1 model (bi2); (c) bidentate binding with Ca1 and Ca3 (bi3); (d) tridentate binding with Ca1 and Ca3 (tri1) in a different manner compared with the bi3 model; (e) tridentate binding with Ca2 and Ca4 (tri2); (f) tridentate binding with Ca2 and Ca4 (tri3) in a reverse model from the tri2 model ; (g) chelate binding with Ca1 (ch1)

Table 2. Adsorption energy (kJ/mol) and O1–C1–O2 bond angle (degree) results of C16Gly adsorbing on the Ca-rich termination of FA (001) surface

Structure	bi1	tri1	bi2	tri2	ch1	bi3	tri13
E_{ads}	-281.1	-272.0	-268.9	-255.3	-245.4	-218.9	-195.2
Bond angle	125.82	124.44	127.59	123.99	124.08	126.22	125.58

between these Ca atoms were all 4.13 Å before the optimization. Due to the surface relaxation, the distance between Ca5 and Ca6 reduced to 4.05 Å, whereas the distances of Ca6–Ca7 and Ca5–Ca7 only increased by 0.01 Å. The variations in the distances between international Ca atoms on this termination arising from the surface relaxation were much less significant compared with those on the Ca-rich termination. These results indicate that the PO₄-rich termination of FA (001) surface is more stable, in line with the fact that the surface energy of PO₄-rich termination is relatively lower than that of the Ca-rich termination.

In the next step, the C16Gly anion was placed on such termination at various initial sites to search the possible binding models. As a result, five low-energy configurations were found as summarized in Fig. 7. The C16Gly anion could react with Ca5 and Ca6 in two different patterns, forming two bidentate structures (bi4 and bi5 structures, Fig. 7a and 7b). Two other bidentate binding models (bi6 and bi7 models) were also found, where Ca6 and Ca7 bonded with the C16Gly anion (Fig. 7c and 7d). Differently, at the top site of Ca7, C16Gly could chelate to Ca7 via two Ca–O bonds (Fig. 7e). Similar to the binding structures on the Ca-rich termination, only O atoms in the carboxyl group of C16Gly could react with the PO₄-rich termination; the O3 of C16Gly failed to interact with a Ca atom on the surface. This finding implies that it is unfavorable for the C16Gly anion to bend over this FA surface and further interact with more Ca atoms.

In the binding models on the PO₄-rich termination, the adjustment of C16Gly anion gave rise to a decrease in the bond angle of O1–C1–O2, except for the bi5 model (Table 3). In the bi5 model, the bond angle of O1–C1–O2 increased by 0.64°. On the other hand, the adsorption energies ranged from -67.6 kJ/mol to -54.8 kJ/mol. Such adsorption energies were an order of magnitude higher compared with those on the Ca-rich termination, indicating that the adsorption of C16Gly anion on the PO₄-rich termination is less favorable.

It should be mentioned that the adsorption energy of C16Gly anion on the dolomite (104) surface is >45 kJ/mol (Cao et al., 2019). The adsorption energies of C16Gly on the Ca-rich or PO_4 -rich termination of FA (001) surface were lower than that on the dolomite (104) surface, suggesting that the adsorption of C16Gly anion on these terminations of FA (001) surface was more stable. This result can be used to explain the selective flotation of FA from dolomite using C16Gly as a collector.

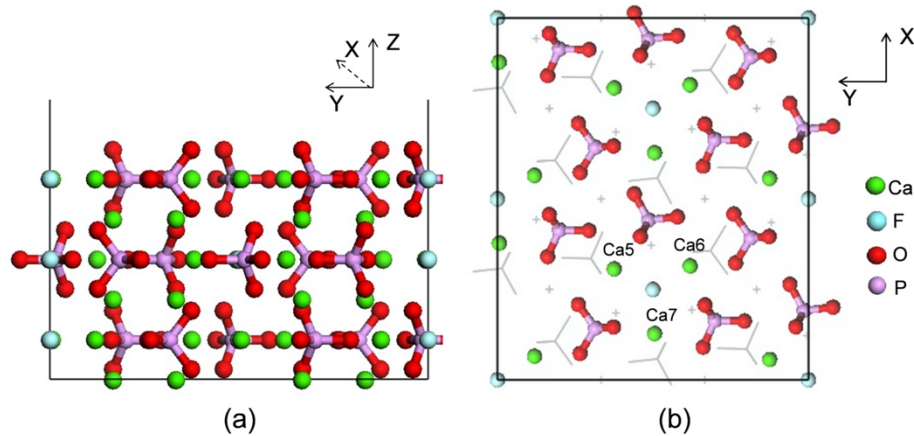


Fig. 6. Optimized PO_4 -rich termination of FA (001) surface: (a) side view and (b) top view (Bottom atoms are showed in a grey-line style)

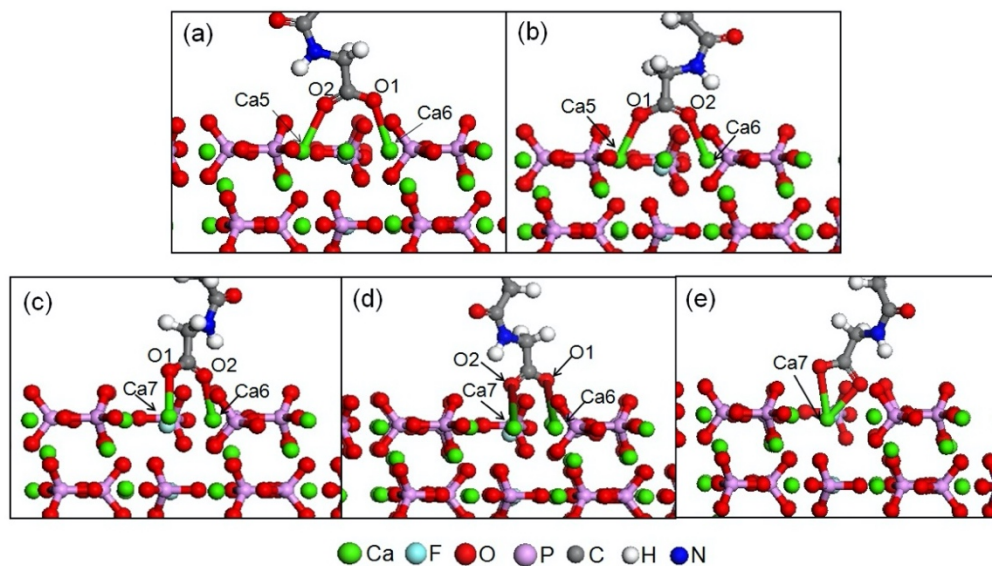


Fig. 7. Binding structures of C16Gly anion on the PO_4 -rich termination of FA (001) surface: (a) bidentate binding with Ca5 and Ca6 (bi4); (b) bidentate binding with Ca5 and Ca6 in a reverse structure from the bi4 model (bi5); (c) bidentate binding with Ca6 and Ca7 (bi6); (d) tridentate binding with Ca6 and Ca7 in a reverse pattern compared with the bi6 model (bi7); (e) chelate binding with Ca7 (ch2)

Table 3. Adsorption energy (kJ/mol) and O1-C1-O2 bond angle (degree) results of C16Gly adsorbing on the PO_4 -rich termination of FA (001) surface

Structure	bi4	ch2	bi5	bi6	bi7
E_{ads}	-67.6	-62.9	-60.00	-56.4	-54.8
Bond angle	130.75	113.19	131.16	126.73	126.95

3.6. Electron density difference analysis

Electron density difference map provides an intuitional visualization of electron transfer among atoms in an interaction, which helps to interpret the bond feature between two interactional atoms. In this

work, we reported the electron density difference results of bi1 and bi4 structures to assess the O–Ca bond natures in these structures, as the bi1 and bi4 models were the most favorable structures of C16Gly anion adsorbing on the Ca-rich and PO₄-rich terminations of FA (001) surface, respectively.

Fig. 8 illustrates the electron density difference slice of selected atoms in the bi1 model. In the slice, the red and blue regions refer to charge accumulation and charge depletion regions, respectively. It was noted that a charge accumulation existed around the O atom in the FA bulk (termed as O_{bulk}). The interaction between the O_{bulk} atom and Ca1 or Ca2 atom caused a minimal effect on the charge distribution in the region between these bonding atoms. This result shows that O_{bulk}–Ca bonds feature a high level of ionicity, in line with the result in a previous report (Yashima et al., 2011). In terms of O2–Ca1 and O1–Ca2 bonds, the formation of these bonds barely changed the charges in the fields around Ca1 and Ca2. It appears that the O2–Ca1 and O1–Ca2 bonds were also typical ionic bonds. In addition, electron transfer was found among the atoms in the C16Gly anion.

Similarly, in the case of bi4 model, the interaction between the C16Gly anion and the PO₄-rich termination could not result in a charge redistribution near Ca5 or Ca6 along the O2–Ca5 and O1–Ca6 bond directions. Therefore, the formed O–Ca bonds in the bi4 model also showed a high level of ionicity. Additionally, as the PO₄ groups were located at higher positions over the Ca atoms on top of the PO₄-rich termination, the electrostatic repulsion force between PO₄ groups and the C16Gly anion did not facilitate the binding of the collector to the FA surface. In this regard, the adsorption of C16Gly anion on the PO₄-rich termination was less favorable than that on the Ca-rich termination.

The above analysis indicated that the interaction between the C16Gly anion and two FA terminations generates ionic Ca–O bonds, resulting in the chemisorption of C16Gly anion on FA surfaces. It should be mentioned that the water molecules on the FA surface were not considered in this work. Water molecules can adsorb on the Ca sites on the fluorite surface (Foucaud et al., 2018a). Moreover, the adsorption energy of collector on the hydrated fluorite surface is different from that on the clean fluorite surface in a vacuum environment (Foucaud et al., 2018b). A similar effect of water molecules may also arise on the FA surface. On the other hand, the dissolution of FA induces Ca²⁺, PO₄³⁻ and F⁻ into the slurry. While, other ions, such as Mg²⁺ from the dissolution of dolomite, are also in the slurry of phosphate ore. These ions can adsorb onto the FA surface, thereby affecting the interaction of the collector with the FA surface (Barrozo et al., 2010). The influence of water molecules and ions on the adsorption of C16Gly is difficult to be evaluated by the DFT method, as this method only can deal with small models (Foucaud et al., 2019a). Further work, such as molecular dynamics simulation, needs to be performed to probe the roles of water molecules and ions (Ca²⁺ and Mg²⁺) on the FA flotation with C16Gly collector.

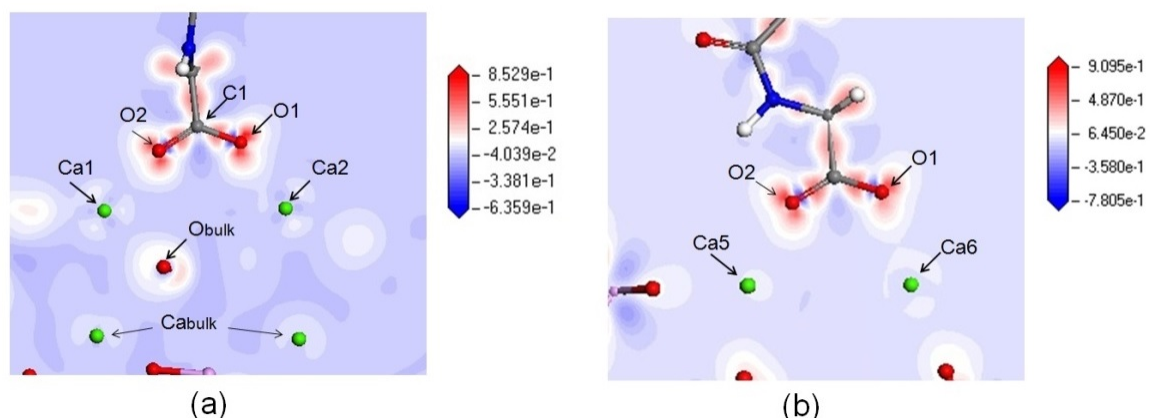


Fig. 8. Electron density difference slices of (a) bi1 and (b) bi4 models

4. Conclusions

C16Gly anion could efficiently adsorb onto the FA surface at pH 9 or 11 to generate a hydrophobic surface. In contrast, the dolomite surface after the condition with the C16Gly solution at the same pH

values still exhibited a high level of hydrophilicity. Thereby, C16Gly can be used as a selective collector for the flotation of FA.

The binding behavior of C16Gly anion on the Ca-rich and PO₄-rich terminations of FA (001) surface highly depended on the steric features of these terminations. In terms of Ca-rich termination, two Ca atoms were located at the outmost layer of the FA surface; the adsorption of C16Gly anion on such surface generated seven binding structures. As for the PO₄-rich termination, the first atomic layer on the surface consisted of the O atoms of PO₄ groups, whereas Ca atoms on the top of the surface were at a relatively deeper layer. The C16Gly anion adsorbed on this surface stably in five configurations. The adsorption of C16Gly anion on the PO₄-rich termination was less stable compared with that on the Ca-rich termination. In all the binding models, only the O atoms in the carboxylic group of C16Gly were involved in the surface reaction, forming Ca–O ionic bonds. The adsorption of C16Gly anion on the PO₄-rich/Ca-rich termination of FA (001) surface is more stable than that on the dolomite (104) surface, which accounts for the selective flotation of FA from dolomite.

Acknowledgments

The financial support provided by the Analysis and Testing Foundation of Kunming University of Science and Technology (China) is gratefully acknowledged.

References

- ALMORABARRIOS, N., AUSTEN, K.F., LEEUW, N.H.D., 2009. *Density Functional Theory Study of the Binding of Glycine, Proline, and Hydroxyproline to the Hydroxyapatite (0001) and (0110) Surfaces*. *Langmuir*, 25, 5018-5025.
- BARROZO, M.A.S., DOSSANTOS, M.A., SANTANA, R.C., CAPPONI, F., ATAIDE, C.H., 2010. *Effect of ionic species on the performance of apatite flotation*. *Sep. Purif. Technol.*, 76, 15-20.
- BORDES, R., HOLMBERG, K., 2011. *Physical chemical characteristics of dicarboxylic amino acid-based surfactants*. *Colloids Surf., A*, 391, 32-41.
- CAO, Q., ZOU, H., CHEN, X., WEN, S., 2019. *Flotation selectivity of N-hexadecanoylglycine in the fluorapatite-dolomite system*. *Miner. Eng.* 131, 353-362.
- CHEN, Y., LIU, M., CHEN, J., LI, Y., ZHAO, C., MU, X., 2018. *A density functional based tight binding (DFTB+) study on the sulfidization-amine flotation mechanism of smithsonite*. *Appl. Surf. Sci.* 458, 454-463.
- FILIPPOV, L.O., FOUCAUD, Y., FILIPPOVA, I.V., BADAWI, M., 2018. *New reagent formulations for selective flotation of scheelite from a skarn ore with complex calcium minerals gangue*. *Miner. Eng.* 123, 85-94.
- FOUCAUD, Y., BADAWI, M., FILIPPOV, L., FILIPPOVA, I., LEBEGUE, S., 2019a. *A review of atomistic simulation methods for surface physical-chemistry phenomena applied to froth flotation*. *Miner. Eng.* 143, 106020.
- FOUCAUD, Y., BADAWI, M., FILIPPOV, L.O., BARRES, O., FILIPPOVA, I.V., LEBEGUE, S., 2019b. *Synergistic adsorptions of Na₂CO₃ and Na₂SiO₃ on calcium minerals revealed by spectroscopic and ab initio molecular dynamics studies*. *Chem.* 10, 9928-9940.
- FOUCAUD, Y., BADAWI, M., FILIPPOV, L.O., FILIPPOVA, I.V., LEBEGUE, S., 2018a. *Surface Properties of Fluorite in Presence of Water: An Atomistic Investigation*. *J. Phys. Chem. B*, 122, 6829-6836.
- FOUCAUD, Y., LEBEGUE, S., FILIPPOV, L.O., FILIPPOVA, I.V., BADAWI, M., 2018b. *Molecular Insight into Fatty Acid Adsorption on Bare and Hydrated (111) Fluorite Surface*. *J. Phys. Chem. B*, 122, 12403-12410.
- FRANCIS, G., PAYNE, M., 1990. *Finite basis set corrections to total energy pseudopotential calculations*. *J. Phys.: Condens. Matter*, 2, 4395.
- GE, Y.Y., GAN, S.P., ZENG, X.B., YU, Y.F., 2008. *Double reverse flotation process of collophanite and regulating froth action*. *Trans. Nonferrous Met. Soc. China*, 18, 449-453.
- GENEYTON, A., FOUCAUD, Y., FILIPPOV, L.O., MENAD, N.E., RENARD, A., BADAWI, M., 2020. *Synergistic adsorption of lanthanum ions and fatty acids for efficient rare-earth phosphate recovery: Surface analysis and ab initio molecular dynamics studies*. *Appl. Surf. Sci.* 526, 146725.
- HEAD, J.D., ZERNER, M.C., 1985. *A Broyden – Fletcher – Goldfarb – Shanno optimization procedure for molecular geometries*. *Chem. Phys. Lett.* 122, 264-270.
- HERRING, J.R., FANTEL, R.J., 1993. *Phosphate rock demand into the next century: Impact on world food supply*. *Nonrenewable Resour.* 2, 226-246.
- HIRVA, P., TIKKA, H.-K., 2002. *Ab initio study on the interaction of anionic collectors with calcite and dolomite surfaces*. *Langmuir*, 18, 5002-5006.

- HU, Y., XU, Z., 2003. *Interactions of amphoteric amino phosphoric acids with calcium-containing minerals and selective flotation*. Int. J. Miner. Process. 72. 87-94.
- KARLKVIST, T., PATRA, A., RAO, K.H., BORDES, R., HOLMBERG, K., 2015. *Flotation selectivity of novel alkyl dicarboxylate reagents for apatite-calcite separation*. J. Colloid Interface Sci. 445. 40-47.
- PENG, C., ZHONG, Y., MIN, F., 2018. *Adsorption of alkylamine cations on montmorillonite (001) surface: A density functional theory study*. Appl. Clay Sci. 152. 249-258.
- PERDEW, J.P., BURKE, K., ERNZERHOF, M., 1996. *Generalized gradient approximation made simple*. Phys. Rev. Lett. 77. 3865.
- PERDEW, J.P., ZUNGER, A., 1981. *Self-interaction correction to density-functional approximations for many-electron systems*. Phys. Rev. B. 23. 5048.
- PRADIP, B, R., 2003. *Molecular modeling and rational design of flotation reagents*. Int. J. Miner. Process. 72. 95-110.
- PRADIP, R, B., RAO, T.K., KRISHNAMURTHY, S., VETERIVEL, R., MIELCZARSKI, J., CASES, J.M., 2002. *Molecular Modeling of Interactions of Alkyl Hydroxamates with Calcium Minerals*. J. Colloid Interface Sci. 256. 106-113.
- QIU, Y.Q., CUI, W.Y., LI, L.J., YE, J.J., WANG, J., ZHANG, Q., 2017. *Structural, electronic properties with different terminations for fluorapatite (0 0 1) surface: A first-principles investigation*. Comput. Mater. Sci. 126. 132-138.
- RAI, B., PRADIP, 2012. *Rational Design of Selective Industrial Performance Chemicals based on Molecular Modelling Computations*, in: Rai, B. (Ed.), *Molecular Modelling for the Design of Novel Performance Chemicals and Materials*. CRC Press, 28-63.
- SEGALL, M., LINDAN, P.J., PROBERT, M.A., PICKARD, C., Hasnip, P., Clark, S., Payne, M., 2002. *First-principles simulation: ideas, illustrations and the CASTEP code*. J. Phys.: Condens. Matter. 14. 2717.
- SIS, H., CHANDER, S., 2003. *Reagents used in the flotation of phosphate ores: a critical review*. Miner. Eng., 16. 577-585.
- WANG, X., NGUYEN, A.V., MILLER, J.D., 2006. *Selective attachment and spreading of hydroxamic acid-alcohol collector mixtures in phosphate flotation*. Int. J. Miner. Process. 78. 122-130.
- YANG, X., LIU, S., LIU, G., ZHONG, H., 2017. *A DFT study on the structure-reactivity relationship of aliphatic oxime derivatives as copper chelating agents and malachite flotation collectors*. J. Ind. Eng. Chem. 46. 404-415.
- YASHIMA, M., YONEHARA, Y., FUJIMORI, H., 2011. *Experimental Visualization of Chemical Bonding and Structural Disorder in Hydroxyapatite through Charge and Nuclear-Density Analysis*. J. Phys. Chem. C. 115. 25077-25087.
- YU, J., GE, Y., GUO, X., GUO, W., 2016. *The depression effect and mechanism of NSFC on dolomite in the flotation of phosphate ore*. Sep. Purif. Technol. 161. 88-95.
- ZHANG, H., HAN, C., LIU, W., HOU, D., WEI, D., 2019. *The chain length and isomeric effects of monohydric alcohols on the flotation of magnesite and dolomite by sodium oleate*. J. Mol. Liq. 276. 471-479.
- ZHANG, J., YANG, W., WANG, J., 2005. *Synthesis of N-Acylglycine Surfactants*. Chem. Ind. Times. 19, 25-27.